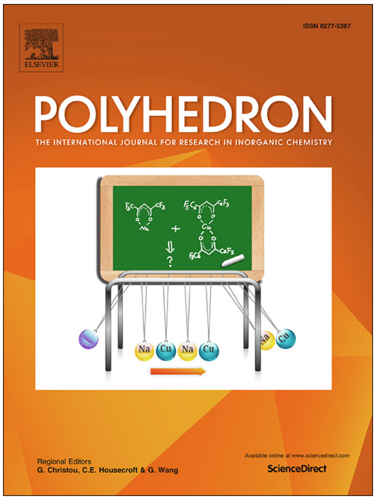

Photophysical, electrochemical and TD-DFT studies of Ni(II) and Mn(II) complexes of N'-(2-furan-3-carbonyl) hydrazine carbodithioic acid ethyl ester

R. Chaurasia, M.K. Bharty, Paras Nath, Piyush Kumar Sonkar, Vellaichamy Ganesan, B. Maiti, A. Bharti, R.J. Butcher

PII: S0277-5387(19)30597-2
DOI: https://doi.org/10.1016/j.poly.2019.114160
Reference: POLY 114160

To appear in: *Polyhedron*

Received Date: 20 June 2019
Revised Date: 19 September 2019
Accepted Date: 20 September 2019

Please cite this article as: R. Chaurasia, M.K. Bharty, P. Nath, P. Kumar Sonkar, V. Ganesan, B. Maiti, A. Bharti, R.J. Butcher, Photophysical, electrochemical and TD-DFT studies of Ni(II) and Mn(II) complexes of N'-(2-furan-3-carbonyl) hydrazine carbodithioic acid ethyl ester, *Polyhedron* (2019), doi: https://doi.org/10.1016/j.poly.2019.114160

REVISED MANUSCRIPT

Photophysical, electrochemical and TD-DFT studies of Ni(II) and Mn(II) complexes of N'-(2-furan-3-carbonyl) hydrazine carbodithioic acid ethyl ester

R. Chaurasia,[a] M.K. Bharty,*[a] Paras Nath,‡[a] Piyush Kumar Sonkar,[a] Vellaichamy Ganesan,[a] B. Maiti,[a] A. Bharti,[b] R. J. Butcher [c]

[a]*Department of Chemistry, Banaras Hindu University, Varanasi-221005, India*
[b]*Department of Chemistry, Kirori Mal College, University of Delhi, Delhi-110007, India*
[c]*Department of Chemistry, Howard University, 525 College Street NW, Washington, DC 20059, USA*

ABSTRACT

Two new complexes [Ni(Hfchce)$_2$(py)$_2$] (**1**) and [Mn(Hfchce)$_2$(*o*-phen)] (**2**) with [N'-(2-furan-3-carbonyl)hydrazine]-carbodithioic acid ethyl ester (H$_2$fchce) have been synthesized which contain *o*-phenanthroline (*o*-phen)/ pyridine (py) as coligand. The ligand and its metal complexes have been characterized by elemental analyses, IR, magnetic susceptibility and single crystal X-ray diffraction data. Complexes **1** and **2** crystallize in orthorhombhic system with space group '*P b c a*' and '*P b c n*', respectively. In complex **1**, nickel centre is coordinated through one hydrazine nitrogen atom, one carbonyl oxygen of two units of ligand and two pyridine nitrogen atoms. The manganese center in complex **2** is coordinated in a N$_4$O$_2$ core by two uininegative bidentate ligands using hydrazine nitrogen (after loss of proton) and carbonyl oxygen and two nitrogen atoms of *o*-phen. In both complexes, the metal ion adopts a distorted octahedral geometry. Complexes **1** and **2** are fluorescent materials which exhibit an emission at 291 and 285 nm, respectively upon excitation at 263 and 251 nm. The course of the thermal degradations of complexes **1** and **2** have been investigated by TGA which indicate that metal oxide is formed as the final residue in both complexes. The metal complexes, [Ni(Hfchce)$_2$(py)$_2$] (**1**) and [Mn(Hfchce)$_2$(*o*-phen)] (**2**) were immobilized on glassy carbon electrodes using Nafion® (Nf). The modified electrodes have been characterized by cyclic voltammetry in 0.1 M KOH. Complexes **1** and **2** have efficient activity towards electrochemical water oxidation in the 0.1 M KOH. The simulated spectra of the two complexes **1** and **2** are characterized by excited states with ligand-to-ligand charge-transfer (LLCT) and ligand-to-metal charge-transfer (LMCT) character.

Keywords: **Keywords:** Ni(II) and Mn(II) complexes, Fluorescence, Electrocatalytic activity, Crystal structure, TD-DFT.

*Corresponding author E-mail: manoj_vns2005@yahoo.co.in; mkbharty@bhu.ac.in

‡ Present address: Department of Chemistry, Buddha P.G. College, Kushinagar, India

1. Introduction

The coordination chemistry of nitrogen, sulphur and oxygen containing ligands is an interesting and emerging area of research [1-4]. The metal complexes formed with nitrogen, sulphur/ oxygen-donor ligands have attracted an increasing interest because of their potential biological and chemical activities [4, 5]. Metal complexes of nitrogen-sulfur containing ligands have attracted a lot of attention of scientists due to their application in the synthesis of bioactive compounds [6]. Metals play a crucial role in various biochemical reactions in therapeutic and diagnostic applications [7]. Metal complexes prepared with these ligands are very interesting from the viewpoint of their semiconducting behaviour, electro-optical, molecular magnetism and electrochemical properties [8-15]. The study of the metal complexes of above types of ligands has profound interdisciplinary relevance because they have several applications in electroactive materials [16]. The S-alkyl/aryl esters derived from potassium salts of N- aroylhydrazine carbodithioates have been found to be more stable towards cyclization as compared to the potassium salt. The potassium salts of N-(aroyl)-hydrazine carbodithioates are not much more stable since they undergo intramolecular cyclization with elimination of H_2S forming 1,3,4-oxadiazole-2-thiones in the presence of weak acid or base [17-19]. The major interest in the synthesis of esters is that they are much more stable than the potassium salt and do not undergo cyclization to form oxadiazole derivatives. Metal-organic compounds comprised of metal ions and bridging ligands have received much attention due to their potential applications as functional materials such as catalysis, gas absorption, molecular recognition and optics [20-22]. Nitrogen-sulfur donor ligands and their metal complexes are efficient catalysts under homogeneous and heterogeneous conditions. The catalytic activity of these catalysts depends on the nature of the substituent as well as the metal centres [23-25]. Therefore, these compounds have been used as catalysts in reactions such as epoxidation of alkenes [26], oxidation of alcohols [27], enantioselective oxidation of sulphides [28, 29], and oxidation of water [30]. Transition metal complexes formed with different metal ions with various oxidation states of Mn(II, IV & VI), Fe(II & III), Co(II & III), Ni(II), and Cu(I & II) involve in the electrochemical water oxidation [30, 31-33]. Nickel complexes are interesting for structural aspects, water oxidation and other important reactions [34-38]. First nickel-based homogeneous water-oxidizing catalyst $[Ni(meso\text{-}L)](ClO_4)_2$ was reported which oxidize water at neutral pH and low overpotential in buffer solution [39].

The electrocatalytic properties and analytical applications of Ni(II) and Mn(II) complexes are not intensively explored. Accordingly, in view of the possible electroanalytical applications, interesting bonding modes, and various other properties exhibited by these type of Ni(II) and Mn(II) complexes. We have synthesized and studied the crystal structures, photoluminescence, thermal behaviour and electrochemical properties, of Ni(II) and Mn(II) complexes of N'-(2-furan-3-carbonyl) hydrazine carbodithioic acid ethyl ester.

2. Experimental Section

2.1 Materials and methods

Commercial reagents were used without further purification and all experiments were carried out in open atmosphere. Isonicotinic acid hydrazide (Sigma Aldrich), CS_2 (S D Fine Chemicals, India) and KOH (Merk) were used as received. Nafion® (Nf) was purchased from Sigma-Aldrich, India (5 wt% solution in lower aliphatic alcohols)**.** N, N'-dimethylformamide (DMF) was procured from S D Fine Chemicals, India. Solutions for all electrochemical experiments were prepared with triple distilled water. All the solvents were purchased from Merk Chemicals, India and used after purification.

2.2. Physical measurements

Carbon, hydrogen and nitrogen contents were estimated on a Carlo Erba 1108 model microanalyser while sulfur was estimated as $BaSO_4$. Magnetic susceptibility measurements were performed at room temperature on a Cahn Faraday balance using $Hg[Co(NCS)_4]$ as the calibrant. Electronic spectra were recorded on a SHIMADZU 1700 UV-Vis Spectrophotometer. Infrared spectra were recorded in the 4000-400 cm^{-1} region as KBr pellets on a Varian Excalibur 3100 FT-IR Spectrophotometer. Thermo-gravimetric analysis (TG-DTA) of complexes **1** and **2** were done using a Perkin Elmer-STA 6000 thermal analyzer, TA Instruments with heating rate of 10, 20 and 30 ^{o}C min^{-1}. ^{1}H and ^{13}C NMR spectra were recorded in DMSO-d_6 on a JEOL AL 500 FT NMR spectrometer using TMS as an internal reference.

2.3 X-ray crystallography

X-Ray diffraction measurements of complexes **1** and **2** were performed on a Oxford Gemini diffractometer equipped with a CrysAlis CCD software package using a graphite mono-chromated Mo Kα (λ= 0.71073 Å) radiation source at 120 (for **1**)/293 K (for **2**). Multi-scan absorption correction was applied to the X-ray data collection for both the complexes. The structures were solved by direct methods (SHELXL-2013) and refined by full matrix least-square on F^2 (SHELXL) using anisotropic displacement parameters for all non-hydrogen atoms. All hydrogen atoms were included in calculated position and refined with a riding model [40]. The MERCURY package and ORTEP-3 for Windows program were used for generating molecular graphics [41, 42].

2.4 Quantum Chemical Calculation

To understand the binding sites and to verify the composition of the complexes, Density Functional Theory (DFT) calculations have been performed. In these calculations, B3LYP density functional theory method has been used which is a hybrid version of DFT and Hartree-Fock (HF) methods [43]. In this method, the exchange energy from Becke's exchange functional is combined with the exact energy from Hartree-Fock theory [44]. The three parameters define the hybrid functional, specifying how much of the exact exchange is mixed in along with the component exchange and correlation functionals [45]. The 6-31G** basis set for all the atoms except metal ions have been used. The LanL2DZ basis set with an effective core pseudo potential has been used for the metal atom [46]. All the geometry optimizations and frequency calculations (to verify a genuine minimum energy structure) were performed using Gaussian 09 program package [47]. The electronic excitation energies and intensities of the three lowest-energy spin allowed transitions were calculated using the time dependent density functional theory (TD-DFT). It is worth pointing out here that the starting geometries were chosen based on X-ray crystallographic structures with required modification for the computations if needed.

2.5 Cyclic Voltammetry

The electrochemical experiments were performed using CH instruments electrochemical workstation (CHI-660C, USA). A one compartment-three electrode electrochemical cell setup which includes glassy carbon (GC) electrode (3 mm diameter), platinum wire and Ag/AgCl (saturated with KCl) electrode as working, counter and reference electrodes, respectively were used for electrochemical experiments. The potentials quoted in this manuscript were referenced to reversible hydrogen electrode (RHE) potential. GC rotating disc electrode (GC-RDE, 5 mm diameter) and RDE setup from Pine research instruments, USA were used for hydrodynamic voltammetry studies.

2.6 Preparation of modified electrode

Nf solution (0.01%) was prepared in ethanol and 14.0 µL of 0.01% Nf solution was coated on a GC electrode and dried for 30 min. The Nf coated GC electrode (GC/Nf) was dipped in 10 mM Ni-Hfchce solution (in DMF) for 1 h. After 1 h, the GC electrode was removed from the dipping solution, rinsed with triple distilled water (abbreviated as GC/Nf/Ni-Hfchce) and used for electrochemical studies. Similar procedure was followed for the preparation of GC/Nf/Mn-Hfchce electrode also.

2.7 Synthesis

2.7.1 Preparation of N'-(2-furan-3-carbonyl) hydrazine carbodithioic acid ethyl ester (H_2fchce)

N'-(2-furan-3-carbonyl)hydrazinecarbodithioic acid ethyl ester (H_2fchce) was synthesized by a mixture of methyl-2-methyl furancarboxylate (2.51 ml, 20 mmol) and hydrazine hydrate (1.0 ml, 20 mmol) in absolute ethanol and refluxed for 4 h. The white crystalline solid obtained upon cooling was filtered off, washed thoroughly with water and finally with diethyl ether and recrystallized from ethanol. The above solid was dissolved in alcoholic solution of KOH and carbon disulphide was added drop wise. After 30 min of stirring, a white precipitate was obtained which was filtered off washed with diethyl ether and dried in vaccuo. Further the precipitate was dissolve in absolute ethanol kept on ice bath and ethyl iodide (1.44 ml, 18 mmol) was added. After 8 h of continuous stirring at room temperature, a yellowish clear solution was obtained which was filtered. The filtrate kept overnight at room temperature and acidified with dilute acetic acid (50%) yellowish solid was filtered off, washed with hot water and recrystallize in ethanol, yield a white crystalline solid. Yield: 60%; m.p. 98 ^{o}C. Anal. found: C = 44.50, H = 5.80, N = 11.65, S = 26.30 (%) Anal. calc. for $C_9H_{12}N_2O_2S_2$ (244.00) C = 44.26, H = 4.91, N =

11.47, S = 26.22%. IR (ν cm^{-1}, KBr): ν(NH) 3294, 3150; ν(C=O) 1645; ν(N–N) 1066s; ν(C=S) 974. ^1H NMR (DMSO-d_6; δ ppm): 11.38 & 10.59 (2H, NH), 7.59–6.87 (m, 2H, furan ring), 3.18 (s, CH_3), 1.38 (q, CH_2), 1.24 (t, CH_3). ^{13}C NMR (DMSO-d_6; δ ppm): 203.81 (C=S), 162.33 (C=O), 109.21–141.77 (furan ring carbons), 29.06 (CH_3 carbon attached with furan ring), 28.25, (CH_2) 14.86 (CH_3). UV-vis (λ_{max}, MeOH, cm^{-1}) 28515 and 29410.

*2.7.2 Synthesis of [Ni(Hfchce)$_2$(py)$_2$] (**1**)*

A solution of freshly prepared ligand N'-(2-furan-3-carbonyl) hydrazine carbodithioic acid ethyl ester (H_2fchce) (0.244 g, 1 mmol) in MeOH (10 ml) was added to a MeOH solution (10 ml) of $NiCl_2.6H_2O$ (0.118 g, 0.5 mmol). This mixture was stirred for 2 h at room temperature. The resulting brown precipitate was filtered off and washed thoroughly with methanol. Few drops of pyridine (0.081 ml, 1 mmol) were added to the methanol-chloroform suspension of the above compound. The resulting reddish-brown clear solution was obtained at room temperature, filtered off and kept for crystallization. Single crystals of the complex suitable for X-ray analysis were obtained by slow evaporation of the above solution over a period of 21 days. Yield: 45%; m.p. 200 ^oC. Anal. found: C = 47.85, H = 4.40, N = 11.70, S = 18.35%. Anal. calc. for $C_{28}H_{32}N_6NiO_4S_4$ (703.54) C = 47.75, H = 4.54, N = 11.93, S = 18.19%. IR (ν cm^{-1}, KBr): ν(N–H) 3067, ν(C=O) 1688; ν(N–N) 1090; ν(C=S) 878, ν(Ni–N) 563, 547; ν(Ni–O) 651. UV-vis (λ_{max}, DMSO, cm^{-1}) 13698 and 15151.

*2.7.3 Synthesis of [Mn(Hfchce)$_2$(o-phen) (**2**)*

A solution of freshly prepared ligand N'-(2-furan-3-carbonyl) hydrazine carbodithioic acid ethyl ester (H_2fchce) (0.244 g, 1 mmol) in MeOH (10 ml) was added to a MeOH solution (10 ml) of $Mn(OAc)_2.4H_2O$ (0.123 g, 0.5 mmol). This mixture was stirred for 1 h at room temperature. The resulting dark-brown precipitate was filtered off and washed thoroughly with ethanol. A methanol solution of *o*-phenanthroline (0.09 g, 0.5 mmol) was added to the methanol-chloroform suspension of the above compound. The resulting yellow clear solution was obtained at room temperature, filtered off and kept for crystallization. Yellow crystals were obtained by slow evaporation of the above solution over a period of 10 days, suitable for single crystal X-ray analysis. Yield: 56%; m.p. 205 ^oC. Anal. found: C = 49.95, H = 4.00, N = 11.50, S = 17.85%. Anal. calc. for $C_{30}H_{30}MnN_6O_4S_4$ (721.78) C = 49.87, H =

4.15, N = 11.63, S = 17.73%. IR (ν cm^{-1}, KBr): ν(NH) 3180, ν(C=O) 1622; ν(N–N) 1087; ν(C=S) 898, ν(Mn–N) 540, 588; ν(Mn–O) 651. UV-vis (λ_{max}, MeOH, cm^{-1}) 28515 and 29410.

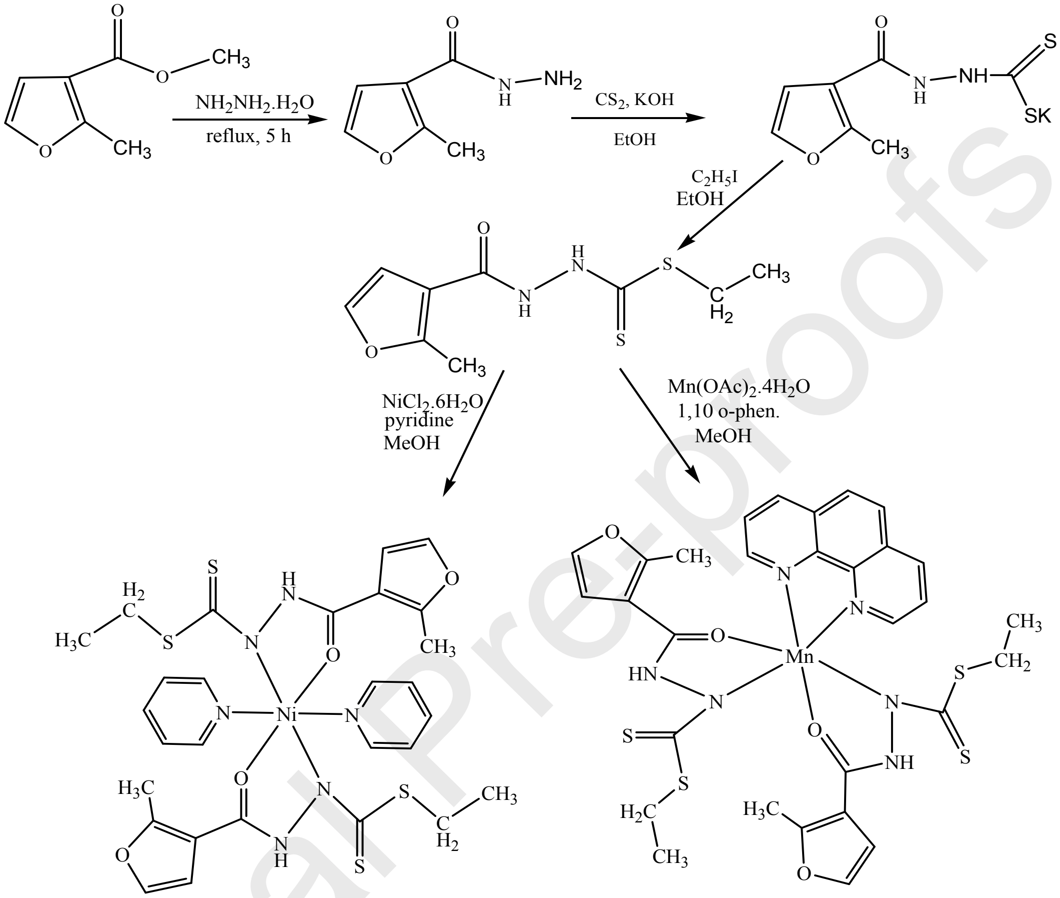

Scheme 1. Preparation of the ligand and its complexes **1** and **2**

3. **Results and discussion**

The ligand N'-(2-furan-3-carbonyl)hydrazine]-carbodithioic acid ethyl ester (H_2fchce) ester reacts with $NiCl_2.6H_2O$ /$Mn(OAc)_2{\cdot}4H_2O$ to form brown and dark-brown precipitates, respectively which dissolve in methanolic solutions of pyridine/ *o*-phen yield [Ni(Hfchce)$_2$(py)$_2$] (**1**) and [Mn(Hfchce)$_2$(*o*-phen)] (**2**). The complexes are stable towards air and moisture. The scheme 1 depicts the formation of the complexes which contain $[\text{Hfchce}]^-$ as ligand and *o*-phen as the coligand. The ligand is soluble in methanol and ethanol while complexes **1** and **2** dissolve in DMF and DMSO. The ligand and complexes **1** and **2** melt at 371, 473 and 478 K, respectively. Single crystal X-ray diffraction data indicate that ligand (H_2fchce) behaves as uninegative, bidentate forming a six member chelate ring. Coordination environment of both complexes is fulfilled by hydrazine nitrogen and carbonyl oxygen of two units of ligand H_2fchce and pyridine/*o*-phen nitrogen donor secondary ligand.

3.1 IR Spectra

The IR spectrum of the ligand N'-(2-furan-3-carbonyl) hydrazine]carbodithioic acid ethyl ester (H_2fchce) shows absorptions due to the stretching modes of NH (3294, 3150 cm^{-1}), C=O (1645 cm^{-1}), N-N (1066 cm^{-1}) and C=S (974 cm^{-1}). The IR spectrum of the complex **1** shows a band at 3067 cm^{-1} indicating the presence of only one NH group upon complexation. The appearance of two new bands for ν(Ni-N) at 547 and 563 and ν(Ni-O) at 663 cm^{-1} suggest bonding of Ni(II) with one carbonyl oxygen, one hydrazinic nitrogen after loss of a proton and pyridine nitrogens. The ν(C=O) and ν(N-N) bands suffer negative and positive shifts of 32 cm^{-1} and 24 cm^{-1}, respectively, indicating that H_2fchce is acting as uninegative bidentate ligand and bonding through carbonyl oxygen and hydrazinic nitrogen in complex **1**. [Mn(Hfchce)$_2$(*o*-phen)] (2) shows the absence of the ν(NH) band at 3294 cm^{-1}, indicating the loss of hydrogen atom from the nitrogen atom of the thioamide group which is supported by a small positive shift of 20 cm^{-1} in ν(N-N). The appearance of three new bands at 540 and 588 and at 651 cm^{-1} due to ν(Ni-N) and ν(Ni-O), suggest bonding through one hydrazinic nitrogen, carbonyl oxygen and both *o*-phen nitrogen atoms. Thus, the H_2fchce acts as a uninegative bidentate in complex **2** [48].

3.2 ^{1}H and ^{13}C NMR spectra

The ^{1}H NMR spectrum of N'-(2-furan-3-carbonyl)hydrazine]-carbodithioic acid ethyl ester (H_2fchce) exhibits two signals at δ 11.38 and 10.59 ppm for the amide and thioamide protons, respectively. Two signals are observed at 1.38 and 1.24 ppm due to CH_2 and CH_3 protons. A signal observed at 3.18 ppm due to CH_3 protons attached with furan ring. Two protons of the furan ring appear as multiplet between δ 7.59-6.87 ppm. The ^{13}C NMR spectrum of H_2fchce shows 9 signals for nine carbons, of which the signals at δ 203.8 and 162.3 ppm are due to the >C=S and >C=O carbons, respectively. The signal for >CH_2 >CH_3 and >CH_3(attached with furan ring) carbons are observed at δ 28.2, 14.8 and 29.0 ppm(methyl carbon attached with furan ring). The furan ring carbons appear in the range of 109.2–141.7 ppm.

3.3 Electronic spectra and magnetic moments

A magnetic moment of 2.91 BM for [Ni(Hfchce)$_2$(py)$_2$] (**1**) and the presence of two bands at 729 and 611 nm assigned to the $^3A_2g \rightarrow ^3T_2g$ (ν_1) and $^3T_1g(F)$ (ν_2) transitions, respectively, suggest a distorted octahedral geometry for the complex **1**. Other two high energy bands observed at 317 and 251 nm may be assigned to intraligand/ charge transfer transitions. [Mn(Hfchce)$_2$(*o*-phen)] (**2**) shows a magnetic moment of 5.9 BM which indicates the presence of five unpaired electrons. It shows two high intensity absorptions at 325 and 263 nm may be assigned to the intraligand/ charge transfer transition (Fig. 1) [49].

3.4 Photoluminescence studies

In the present work, we have examined the photoluminescence properties of ligand H$_2$fchce, complexes [Ni(Hfchce)$_2$(py)$_2$] (**1**) and [Mn(Hfchce)$_2$(*o*-phen)] (**2**) at room temperature. Ligand H$_2$fchce displays an emission at 291 nm upon excitation at 246 nm. Complex **1** shows photoluminiscence at 292 nm upon excitation at 251 nm. The complex **2** upon excitation of at 263 nm, the corresponding emission was observed at 285 nm (Fig. 2). Photoluminescence studies indicate that the both complexes are better fluorescent material as compared to the ligand. The excitation spectra of complexes **1** and **2** show maxima at 292 nm and 285 nm which are close to those observed in the absorption spectra.

3.5 Thermal studies

The thermal properties of complexes **1** and **2** were studied by TG-DTA under a nitrogen atmosphere in the temperature range 25-800 ºC at controlled heating rate of 5 ºC min^{-1}. The TG-DTA curves of complexes **1** and **2** are shown in Fig. 3. The complexes **1** and **2** are thermally stable up to 190 °C and 140 °C, respectively. The decomposition of the organic part of the complex **1** occurs in the temperature range 190-800 °C during which 88.50% weight loss was observed (calc. 89.39%). The first weight loss at 190 °C corresponds to the endothermal decomposition of the pyridine molecules (Obs; 20.95%, calc. 20.75 %). The corresponding endothermic peak of this decomposition was observed in DTA curve at 190 °C. The decomposition of remaining organic moiety was observed in the temperature range

200-800 °C with the weight loss of 65.55% (calc. 68.64%). The decomposition of complex **2** occurs at the temperature range of 140-800 °C during which 89.94% weight loss was observed (calc. 90.16%). The first weight loss of 68.50% at 140 °C corresponds to thermal decomposition of two ligand moieties (calc. 67.68%) with a significant exothermic effect at 180 °C. In second decomposition, the weight loss of 23.25% (calc. 24.99 %) was observed corresponds to the release of *o*-phen molecule. Finally at higher temperature (800 °C), the metal is converted into the metal oxide in complexes **1** (obs. 11.50%, calc. 10.61%) and **2** (obs. 10.06%, calc. 9.84%). Comparing the TG-DTA curves, it was observed that the major weight loss process started after the melting temperature of both complexes.

*3.6 Crystal structure description of [Ni(Hfchce)$_2$(py)$_2$] (**1**)*

Figure 4 shows an ORTEP diagram of complex **1** with the atomic numbering scheme. The structural refinement data related to complex **1** are listed in Table 1, the selected bond distances and bond angles are listed in Table 2. The metal center in complex **1** is coordinated in an N_4O_2 core by two uninegative bidentate ligands using hydrazine nitrogen and carbonyl oxygen. The distances found within the chelate rings are intermediate between single and double bond lengths. The average bond lengths in complex **1** are: O1-C6 = 1.252(3), N3-C6 = 1.325(3), N2-N3 = 1.391(3)Å which suggest considerable delocalization of charge [50]. The nitrogen/oxygen donor sites of the bidentate ligand chelates the Ni(II) center to form a five-membered CN_2ONi ring. The resulting complex has a distorted octahedral geometry. The arrangement of pyridine is *trans* which makes less distorted geometry in complex **1.** The Ni-O bond length in the complex is 2.051 Å and the Ni-N bond lengths are 2.134 and 2.084 Å for Ni-N (hydrazinic) and Ni-N (pyridine), respectively. The longer Ni-N (hydrazinic) bond length as compared to Ni-N (pyridine) indicates that the pyridine nitrogen bonds more strongly than the hydrazine nitrogen. The bond angles O(1)-Ni-N(2) 100.48(8), O(1)-Ni-N(2) 79.52(8) and O(1)-Ni-N(1) 89.32(8)º indicate distortion from an ideal octahedral geometry [51]. The bond distances C(7)-N(2) and C(6)-N(3) show partial double bond character due to delocalization of π electrons throughout the whole chelate ring in the complex [52]. Both chelate rings around Ni(II)centre formed by the $(Hfchce)^-$ are almost planar to each other. In complex, the chelate rings and the pyridine rings are perpendicular to each other forming a dihedral angle of 83.81º. In the solid state, complex **1** is stabilized by weak intermolecular C-H···S interaction (Table 4) between thioether sulfur of one molecule and pyridine ring hydrogen atom of nearby molecule (Fig. 5).

*3.7 Crystal structure description of [Mn(Hfchce)$_2$(o-phen)] (**2**)*

Figure 6 shows an ORTEP diagram of complex **2** together with the atom numbering scheme. The structural refinement data related to complex **2** are listed in Table 1 and the selected bond distances and bond angles are listed in Table 3. The (N, O) donor sites of the uninegative bidentate ligand chelates the Mn(II) center to form a five-membered CN_2OMn ring. The average bond lengths in complex **2** are: O2-C6 = 1.301(12), N1-C6= 1.330(3), N1-N2 = 1.387(3), N2-C7 = 1.319(3) Å which suggest considerable delocalization of charge. The geometry of the resulting complex is a distorted octahedral. In complex **2,** the arrangement of *o*-phen makes *cis* chelate ring, such arrangement possibly makes more distorted geometry. In metal complexes bonding of the ligand takes place through carbonyl oxygen, nitrogen and also bonded with N-heterocyclic bases such as *o*-phen or bpy are prone to exhibit metalloaromaticity [53], but in both the complexes do not observe such behaviour. The bond distances for Mn-O, Mn-N and Mn-N(phen) are 2.171(15), 2.260(19) and 2.280(19) Å, respectively which are comparable to the bond lengths reported for $[Mn_3(O_2CCH_3)_6(N\text{-}N)_2]$ (where N-N = *o*-phen) [54] and $[Mn_2(phen)(Hdcbi)]n$ (Hdcbi = 4,5-dicarboxyimidazole) [55]. The crystal of complex **2** is stabilized by weak intramolecular N-H···S interaction between thioether sulfur of one molecule and hydrazine hydrogen. In addition, an intermolecular C-H···S interaction (Table 5) occurs between CH hydrogen atoms of ethyl group and thioether sulfur atoms of ligand leading to butter like structure which also stabilizes the structure of complex **2** (Fig. 7).

3.8 DFT calculations

Slight disagreements in the observed and calculated bond lengths, C7-S1=1.698 $(1.707)_{calc}$; C6-O1=1.252 $(1.279)_{calc}$; Ni-N1=2.084 $(1.945)_{calc;}$ Ni-O1=2.051 $(1.909)_{calc}$ for $[Ni(Hfchce)_2(py)_2]$ (**1**) and Mn-O2=2.172 $(2.180)_{calc}$; Mn-N2= 2.260 $(2.402)_{calc}$ S1-C7=1.687 $(1.669)_{calc;}$ C6-O2=1.250 $(1.254)_{calc}$ for [Mn(Hfchce)$_2$(*o*-phen)] (**2**) may be due to the fact that the DFT calculations are for an isolated molecule in the gas phase, while the

X-ray crystallographic data were obtained from the crystal lattice. Nevertheless, there is generally good agreement between the geometrical parameters obtained by X-ray crystallography to those generated by the DFT method (Table 2).

3.8.1 TD-DFT Calculation:

The geometric parameters computed with B3LYP and Hartree-Fock (HF) methods were found to be in good agreement with the corresponding experimental values. For reference we have computed absorption bands of the free ligand. Our TD-DFT calculation showed two bands at 246 and 284 nm, which are very comparable to experimental observed bands at 246 and 291 nm, respectively. The experimentally observed absorption bands of the complexes $[Ni(Hfchce)_2(py)_2]$ (**1**) $[Mn(Hfchce)_2(o\text{-}phen)]$ (**2**) have also been explained with the help of TD-DFT calculations. As observed, the TD-DFT prediction of the experimental absorption spectrum matches very well, and from those theoretical calculations the assignment of the character of these transitions can be proposed. Since each absorption line in a TD-DFT spectrum is due to several single excitations, a depiction of the transition character is generally not straightforward. Calculations indicate that complex $[Ni(Hfchce)_2(py)_2]$ (**1**) shows a band at 319 nm which can be compared with experimentally observed band at 317 nm in MeOH solution. The calculated band at 319 nm with oscillator strengths *(f)* 0.2263 is assigned to the ligand to ligand charge transfer transitions from the coordinated ligand moiety to the five membered furan ring of the ligand (Fig.8) associated with the transitions HOMO-1 to LUMO+4 (91.6%) and HOMO to LUMO+3 (4%). In the case of complex $[Mn(Hfchce)_2(o\text{-}phen)]$ (**2**), the electronic absorption spectrum displayed one band at 327 nm which can be compared with the experimentally observed band at 325 in MeOH solution (Fig.9). Quantum chemical calculations reveal that the band calculated at 327 nm with oscillator strength (*f*) 0.1405. This band is a combination eighteen individual transitions. For clarity, however, we have shown only three more dominant transitions involving HOMO to LUMO+2 (5%), HOMO-1 to LUMO+4 (8%) and HOMO to LUMO+4 (2%). These transitions indicate that electron transfer from the coordinated sulfur atoms of the ligand [N'-(2-furan-3-carbonyl) hydrazine]-carbodithioic acid ethyl ester (H_2fchce) with slight intermingling of the metal d-electrons to the chelate ring.

3.9 Electrochemical characterizations

The modified electrodes, GC/Nf/Ni-Hfchce and GC/Nf/Mn-Hfchce are tested in 0.1 M KOH using cyclic voltammetry (Fig. 10A). GC and GC/Nf electrodes do not indicate any redox signals in 0.1 M KOH at a scan rate of 20 mVs^{-1}. GC/Nf/Ni-Hfchce shows oxidation and reduction signals at 1.44 and 1.36 V (*vs.* RHE), correspond to Ni(II)/Ni(III) and Ni(III)/Ni(II) electrochemical process, respectively [56-58]. However, GC/Nf/Mn-Hfchce displays a broad peak at 1.55 V, (*vs.* RHE) with very low current indicating a weak oxidation process in the basic medium [59-61]. The modified electrodes are further tested for water oxidation in the basic medium (*vide infra*).

3.9.1 Electrochemical water oxidation

Analysis of electrochemical water oxidation is performed using Linear Sweep Voltammetry (LSV) with a GC-RDE in 0.1 M KOH at the scan rate of 5 mVs^{-1} (Fig. 10B). It is observed that the GC-RDE and GC-RDE/Nf electrodes show inefficient water oxidation at 1.78 and 1.80 V (*vs.* RHE), respectively. The GC-RDE/Nf/Ni-Hfchce and GC-RDE/Nf/Mn-Hfchce electrodes represent oxidation signals attributed to water oxidation at 1.51 and 1.64 V (*vs.* RHE), respectively. The oxidation current obtained at GC-RDE/Nf/Ni-Hfchce is higher than GC-RDE/Nf/Mn-Hfchce, GC-RDE/Nf and GC-RDE electrodes. Efficiency of the water oxidation can be determined by the potential required to achieve a current density of 10 mA cm^{-2}. The 10 mA cm^{-2} current has been observed for GC-RDE/Nf/Ni-Hfchce at 1.72 V (*vs.* RHE), which is very close to the potential exhibited by commercial catalysts (20% Pt/C = 2.02, 20% Ru/C=1.62 and Ir/C= 1.61) [62]. and other reported cobalt based catalysts [63]. These results suggest that the GC-RDE/Nf/Ni-Hfchce electrode has efficient electrochemical activity towards water oxidation. Thus GC-RDE/Nf/Ni-Hfchce electrode may be useful for regenerated fuel cells which utilize oxygen reduction and oxygen evolution reactions, water electrolysis and metal air batteries [62, 64-66].

4. Conclusions

A new ligand [N'-(2-furan-3-carbonyl)hydrazine]-carbodithioic acid ethyl ester (H_2fchce) and its complexes [Ni(Hfchce)$_2$(py)$_2$] (**1**) and [Mn(Hfchce)$_2$(*o*-phen)] (**2**) have been synthesized. The arrangement of pyridine is *trans* in complex **1** while in complex **2** *o*-phen makes *cis* chelate ring, such an arrangement possibly makes complex **2** have much more distorted geometry than complex **1**. Complexes **1** and **2** are better fluorescent as compared to free ligand and showed emission band at 292 and 285 nm upon excitation at 251 and 263 nm, respectively. TD-DFT prediction of the experimental absorption spectrum matches very well. The crystal structure of the complexes are stabilized through weak intermolecular C-H···S and intramolecular N-H···S interactions leading to a supramolecular architecture. The Ni-Hfchce and Mn-Hfchce complexes are successfully immobilized on the GC electrode. GC/Nf/Ni-L and GC/Nf/Mn--Hfchce have efficient activity for water oxidation. Out of these electrodes, GC/Nf/Ni-Hfchce has outstanding performance for the water oxidation in the basic medium. The GC/Nf/Ni-Hfchce could be a suitable alternative for the commercial OER catalysts used in water splitting, regenerated fuel cells and rechargeable metal-air batteries.

5. Acknowledgement

Dr. M. K. Bharty is thankful to the Science and Engineering Research Board, India for the award of young scientist project (No. YSS/2015/001201).

6. Supplementary material

CCDC 1412088 and 1905731 contain the supplementary crystallographic data for the complexes **1** and **2**. These data can be obtained free of charge *via* http://www.ccdc.cam.ac.uk/ conts/ retrieving.html, or from the Cambridge Crystallographic Data Centre, 12 Union Road, Cambridge CB2 1EZ, UK; fax: (+44) 1223-336-033; or e-mail: deposit@ccdc.cam.ac.uk.

References

[1] A. Kobayashi, E. Fujiwara, H. Kobayashi, Chem. Rev. 104 (2004) 5243-5264.

[2] M.K. Bharty, R.K. Dani, N.K. Singh, R.J. Butcher, Polyhedron 112 (2016)-67-77.

[3] N.M. El-Metwally, I.M. Gabr, A.A. El-Asmy, Trans. Met. Chem. 31 (2006) 71-78.

[4] R.K. Dani, M.K. Bharty, S.K. Kushawaha, O. Prakash, V.K. Sharma, R.N. Kharwar, R.K. Singh, N.K. Singh, Polyhedron 81 (2014) 261-172.

[5] A. H. Abu, M.D. Darawsheh, E. Rappocciolo, Polyhedron 61 (2013) 235-241.

[6] K. H. Thompson, Encyclopedia of Inorganic Chemistry. In: King RB (ed.), John Wiley & Sons Ltd., Chichester, UK (2011).

[7] K. H. Thompson and C. Orvig, Science 300 (2003) 936-939.

[8] A. Kobayashi, E. Fujiwara and H. Kobayashi, Chem. Rev. 104 (2004) 5243-5264.

[9] N. Robertson and L. Cronin, Coord. Chem. Rev. 227 (2002) 93-127.

[10] G. Hogarth, Prog. Inorg. Chem. 53 (2005) 71-561

[11] V. Singh, R. Chauhan, A. Kumar, L. Bahadur, N. Singh, Dalton Trans. 39 (2010) 9779-9788.

[12] W. Paw, S. D. Cummings, M. A. Mansour, W. B. Connick, D. K. Geiger and R. Eisenberg, Coord. Chem. Rev. 171 (1998) 125-150.

[13] H. Struthers, T. L. Mindt and R. Schibli, Dalton Trans. 39 (2010) 675-696.

[14] A. Otero, J. Ferna´ndez-Baeza, A. Antin˜olo, J. Tejeda and A. Lara-Sa´nchez, Dalton Trans. (2004) 1499-1510.

[15] J. C. M. Rivas, E. Salvagni, R. Prabaharan, R. T. M. de Rosales and S. Parsons, Dalton Trans. (2004) 172-177.

[16] S. Paswan, M. K. Bharty, P. Bharati, P. K. Sonkar, V. Ganesan and R. J. Butcher, New J. Chem. 41 (2017) 15466-15474.

[17] M. K. Bharty, A. Bharti, R. K. Dani, R. Dulare, P. Bharati and N. K. Singh, J. Mol. Struct. 1011 (2012) 34–41.

[18] N. K. Singh, S. K. Kushawaha, M. K. Bharty, R. Dulare and R. J. Butcher, J. Mol. Struct. 936 (2009) 257-263.

[19] N. K. Singh, M. K. Bharty, S. K. Kushawaha, U. P. Singh and P. Tyagi, Polyhedron 29 (2010) 1902-1909.

[20] Z. H. Zhang, C. P. Li, Y. L. Tian and Y. M. Guo, Inorg. Chem. Commun. 11 (2008) 326-329.

[21] G. Mahmoudi and A. Morshli, Cryst. Eng. Commun. 9 (2007) 1062-1072.

[22] S. R Batten and R. Robson, Angew. Chem., Int. Ed. 37 (1998) 1460-1494.

[23] S. Rayati, E. Khodaei, M. Jafarian, A. Bahrami, A. Wojtczak and A. Kozakiewicz, J. Coord. Chem. 70 (2017) 1424-1437.

[24] K. C. Gupta and A. K. Sutar. Coord. Chem. Rev. 252 (2008) 1420-1450.

[25] K. C. Gupta, A. K. Sutar and C. C. Lin. Coord. Chem. Rev. 253 (2009) 1926-1946.

[26] G. Grivani, A. D. Khalaji, V. Tahmasebi, K. Gotoh and H. Ishida, Polyhedron 31 (2012) 265-271.

[27] S. J. Lippard and J. M. Berg, Principles of Bioinorganic Chemistry (1994) University Science Books, California.

[28] M. Amini, A. Arab, R. Soleyman, A. Ellern, L.K. Woo. J. Coord. Chem. 66 (2013) 3770-3781.

[29] N. Khadir, M. Amini, A. Assoud, M. Bagherzadeh, D. M. Boghaei. J. Coord. Chem. 69 (2016) 103-111.

[30] H. Feizi, F. Shiri, R. Bagheri, J. P. Singh, K. H. Chae, Z. Song and M. M. Najafpour, Catal. Sci. Technol. 8 (2018) 3954-3968.

[31] M. M. Najafpour, G. Renger, M. Hołyńska, A. N. Moghaddam, E. -M. Aro, R. Carpentier, H. Nishihara, J. J. Eaton-Rye, J. -R. Shen and S. I. Allakhverdiev, Chem. Rev. 116 (2016) 2886–2936.

[32] W. Rüttinger and G. C. Dismukes, Chem. Rev. 97 (1997) 1-24.

[33] J. P. McEvoy and G. W. Brudvig, Chem. Rev. 106 (2006) 4455–4483.

[34] S. Sarkar, S. K. Nag and A. P. Chattopadhyay, K. Dey, S. M. Islam, A. Sarkar and S. Sarkar, J. Mol. Struct. 1160 (2018) 9-19.

[35] Y. Cao, M. Lu, J. Fang, L. Shi and D. Zhang, Chem. Commun. 53 (2017) 7549-7552.

[36] Y. Han, Y. Wu, W. Lai and R. Cao, Inorg. Chem. 54 (2015) 5604–5613.

[37] M. M. Najafpour and H. Feizi, Dalton Trans. 41 (2012) 10292–10297.

[38] N. D. Schley, J. D. Blakemore, N. K. Subbaiyan, C. D. Incarvito, F. D'Souza, R. H. Crabtree and G. W. Brudvig, J. Am. Chem. Soc. 133 (2011) 10473–10481.

[39] M. Zhang, M. T. Zhang, C. Hou, Z. F. Ke and T. B. Lu, Angew. Chem., Int. Ed. 53 (2014) 13042–13048.

[40] G. M. Sheldrick, Acta Crystallogr. Section A 64 (2008) 112-122.

[41] C. F. Macrae, I. J. Bruno, J. A. Chisholm, P. R. Edgington, P. McCabe, E. Pidcock, L. Rodriguez-Monge, R. Taylor, J. van de Streek and P. A. Wood, J. Appl. Cryst. 41 (2008) 466-470.

[42] L. J. Farrugia, J. Appl. Cryst. 49 (2012) 849-854.

[43] L. J. Bartolottiand, K. Fluchick, in Reviews in Computational Chemistry, ed. K. B. Lipkowitz, D. Boyd, VCH, New York 7 (1996) 187-216.

[44] A. D. Becke, J. Chem. Phys. 98 (1993) 5648-5652.

[45] C. Lee, W. Yang and R. G. Parr, Phys. Rev. B: Condens. Matter 37 (1988) 785-789.

[46] P. J. Hay and W. R. Wadt, J. Chem. Phys. 82 (1985) 270-283.

[47] M. J. Frisch et al. Gaussian 09, Revision C.01; Gaussian, Inc., Wallingford CT, (2009).

[48] K. Nakamoto, Infrared and Raman Spectra of Inorganic and Coordination Compounds (1986) fourth ed., Wiley Interscience, New York.

[49] A. B. P. Lever, Inorganic Electronic Spectroscopy, second ed., Elsevier, Amsterdam (1984).

[50] J. R. Dilworth, J. Hyde, P. Lyford, P. Vella, K. Venkatasubramaman and J. A. Zubieta, Inorg. Chem. 18 (1979) 268-274.

[51] A. Sreekanth, U. L. Kala, C. R. Nayar and M. R. P. Kurup, Polyhedron 23 (2004) 41-47.

[52] S. Roy, T. N. Mandal, A. K. Barik, S. Pal, S. Gupta, A. Hazra, R. J. Butcher, A. D. Hunter, M. Zeller and S. K. Kar, Polyhedron 26 (2007) 2603-2611.

[53] M. Calvin and K. W. Wilson, J. Am. Chem. Soc. 67 (1945) 2003-2007.

[54] S. G. Baca, Y. Sevryugina, R. Clerac, I. Malaestean, N. Gerbeleu and M. A. Petrukhina, Inorg. Chem. Comm. 8 (2005) 474-478.

[55] X. Zhang, D. Huang, F. Chen, C. Chen and Q. Liu, Inorg. Chem. Comm. 8 (2004) 662-665.

[56] J. Losada, I. Del Peso and L. Beyer, Journal of Electroanalytical Chemistry 447 (1998) 147-154.

[57] I. Santos, M. Vilas-Boas, M. Piedade, C. Freire, M. T. Duarte and B. de Castro, Polyhedron 19 (2000) 655-664.

[58] A. Singh, S. L. Chang, R. K. Hocking, U. Bach and L. Spiccia, Catalysis Science & Technology 3 (2013) 1725-1732.

[59] A. J. Bard, L. R. Faulkner, J. Leddy and C. G. Zoski, Electrochemical methods: fundamentals and applications, Wiley New York 2 (1980).

[60] M. M. Najafpour and S. I. Allakhverdiev, International Journal of Hydrogen Energy 37 (2012) 8753-8764.

[61] M. M. Najafpour, F. Rahimi, E.-M. Aro, C.-H. Lee and S. I. Allakhverdiev, Journal of the Royal Society Interface 9 (2012) 2383-2395.

[62] Y. Gorlin and T. F. Jaramillo, Journal of the American Chemical Society 132 (2010) 13612-13614.

[63] L. Han, S. Dong and E. Wang, Advanced Materials 28 (2016) 9266-9291.

[64] A. T. Aqueel Ahmed, B. Hou, H. S. Chavan, Y. Jo, S. Cho, J. Kim, S. M. Pawar, S. Cha, A. I. Inamdar and H. Kim, Small 14 (2018) 1870132.

[65] X. Xiong, Y. Ji, M. Xie, C. You, L. Yang, Z. Liu, A. M. Asiri and X. Sun, Electrochemistry Communications 86 (2018) 161-165.

[66] J. S. Sagu, D. Mehta and K. U. Wijayantha, Electrochemistry Communications 87 (2018) 1-4.

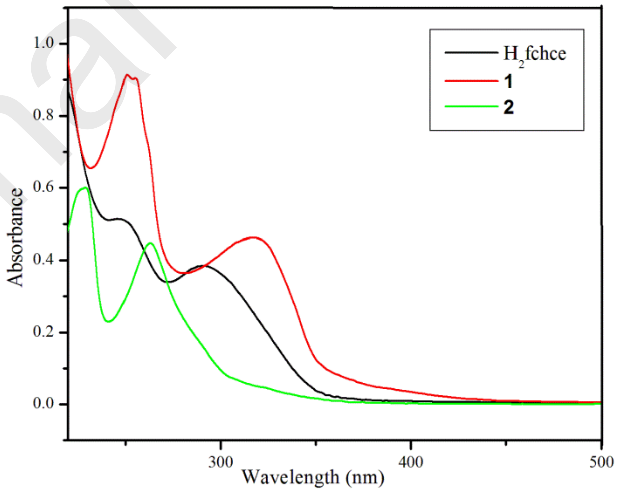

Fig.1. UV-vis. absorption spectra of H_2fchce and complexes **1** and **2** at 10^{-3} M in MeOH

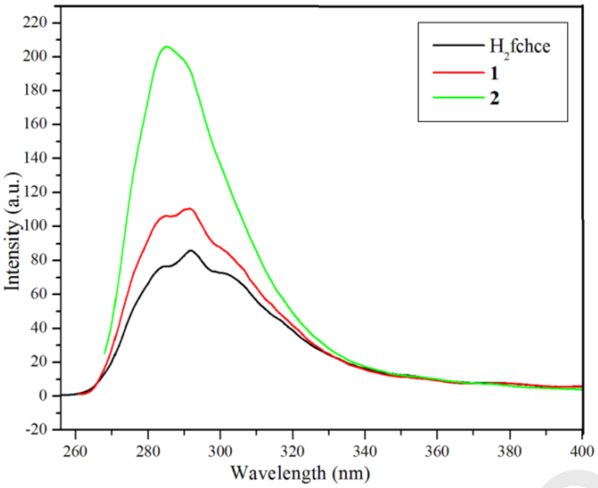

Fig. 2. Emission spectra of H$_2$fchce and complexes **1** and **2** at 10^{-5} M in MeOH. (Excitation wavelength for H$_2$fchce and its complexes **1** and **2** are 246, 251 and 263 nm)

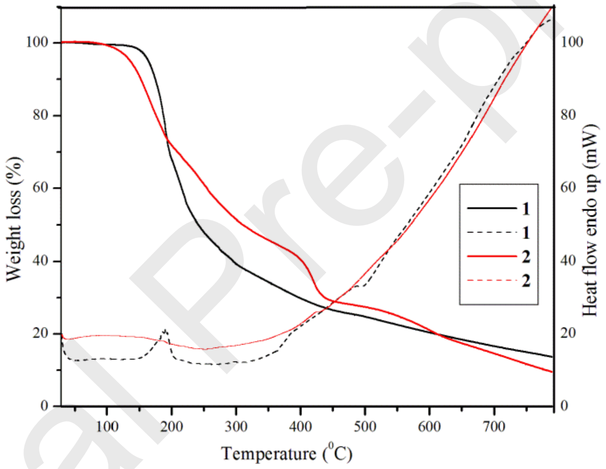

Fig. 3. TG-DTA curves showing the thermal degradation of complexes **1** and **2**, at 5 ^oC min^{-1} in N$_2$ atmosphere (TGA curves are shown in solid lines & DTA in dotted)

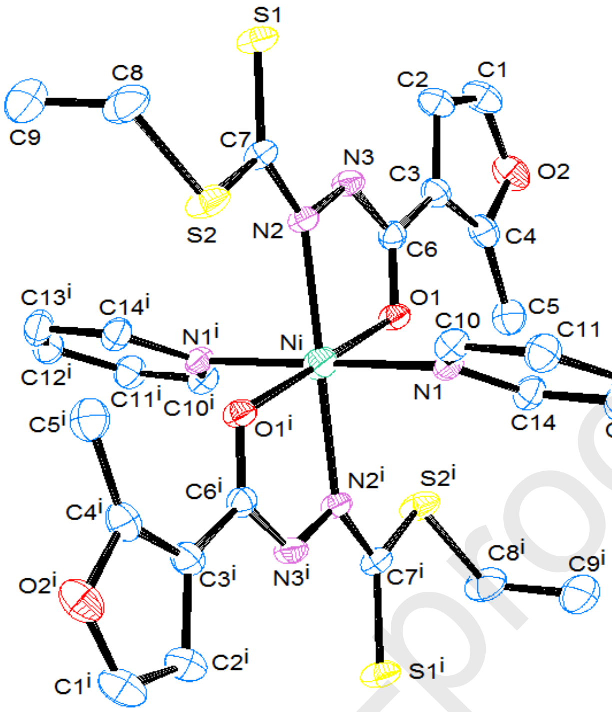

Fig. 4. ORTEP diagram of [Ni(Hfchce)$_2$(py)$_2$] (**1**)

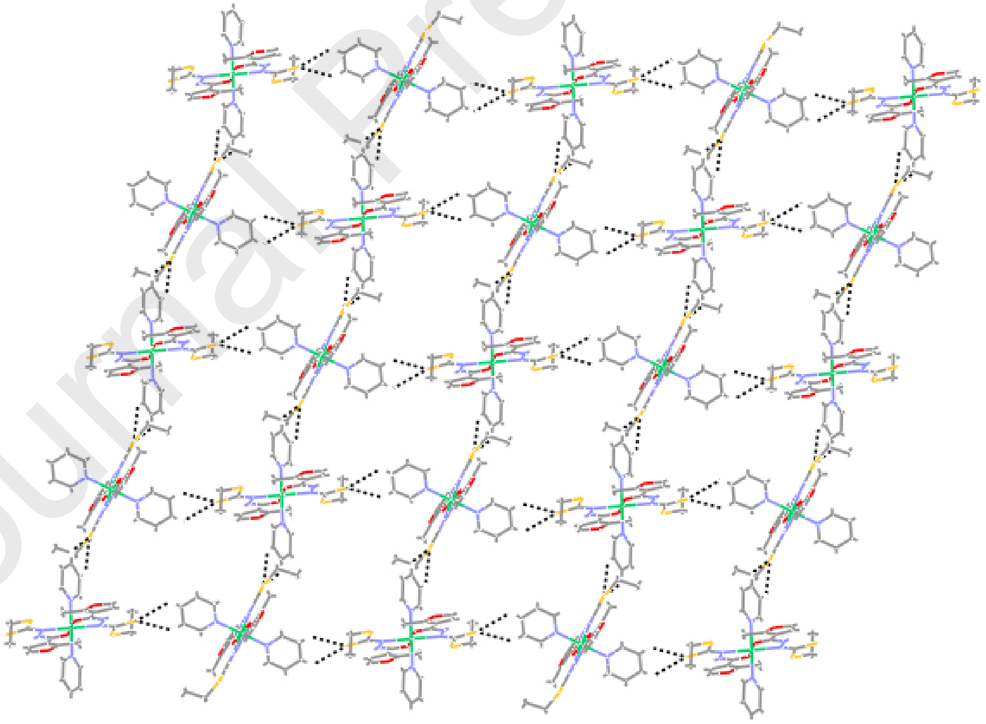

Fig. 5. Showing intermolecular C-H···S hydrogen bonding leading to a linear chain structure in complex **1**

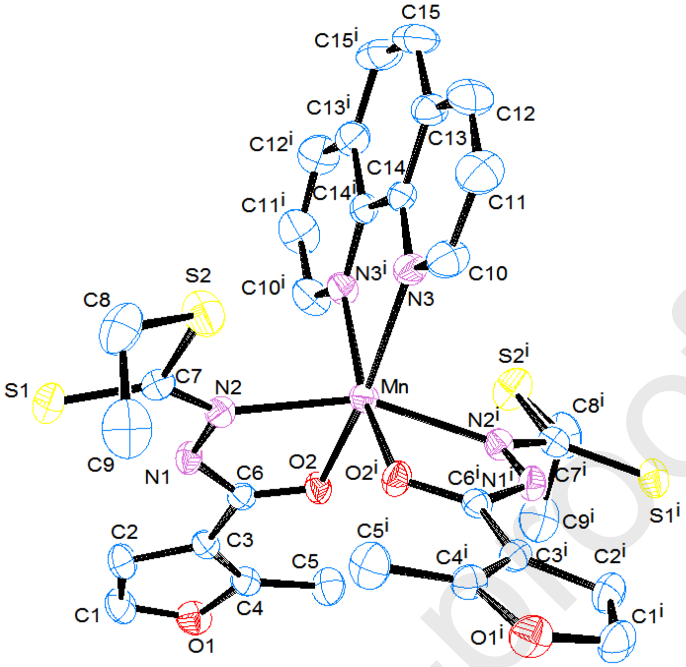

Fig.6. ORTEP diagram of [Mn(Hfchce)2(o-phen)] (2) at 30 % probability level.

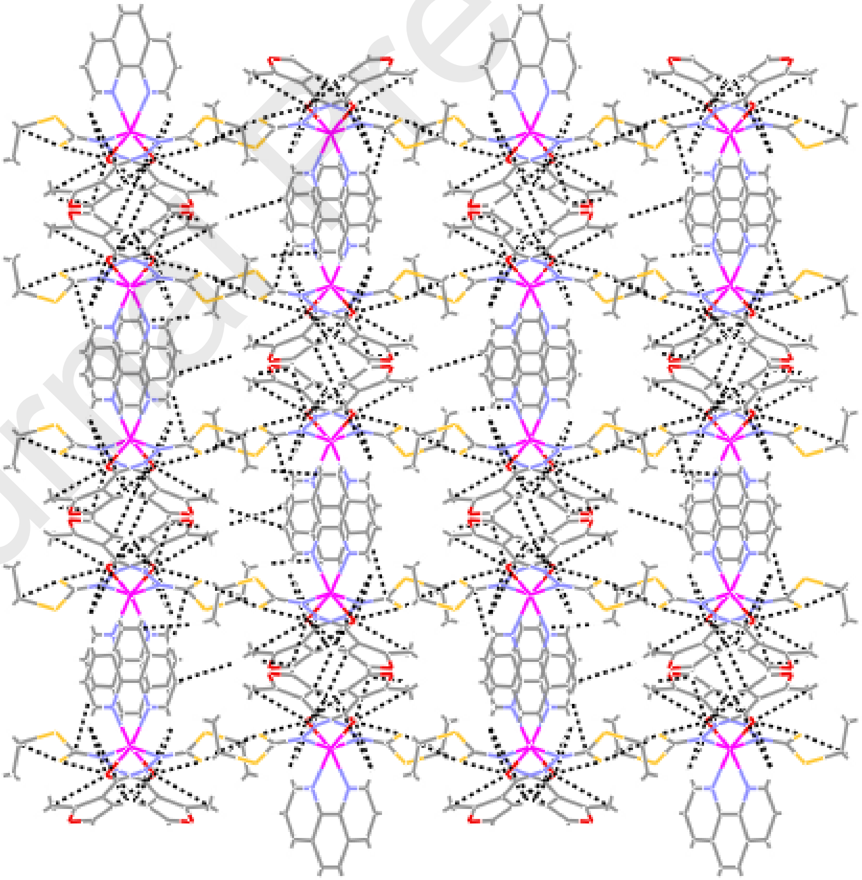

Fig. 7. Showing intramolecular C-H···S hydrogen bonding leading to a butter like structure in complex **2**

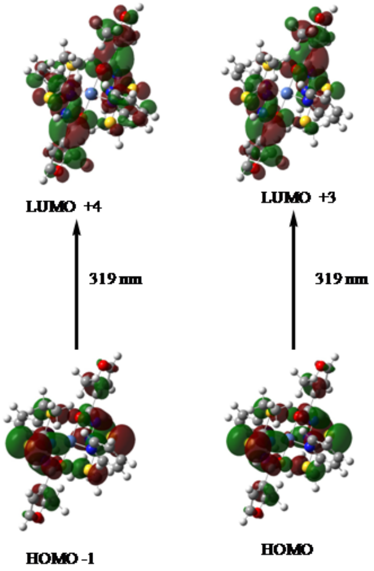

Fig. 8. Electronic transitions of selected molecular orbitals for complex **1**

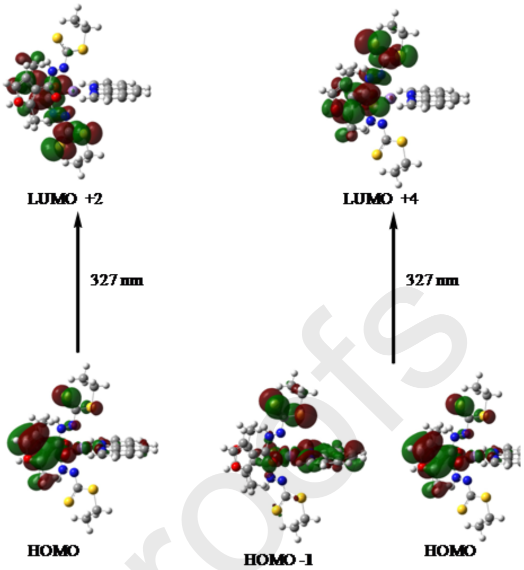

Fig. 9. Electronic transitions of selected molecular orbitals for complex **2**

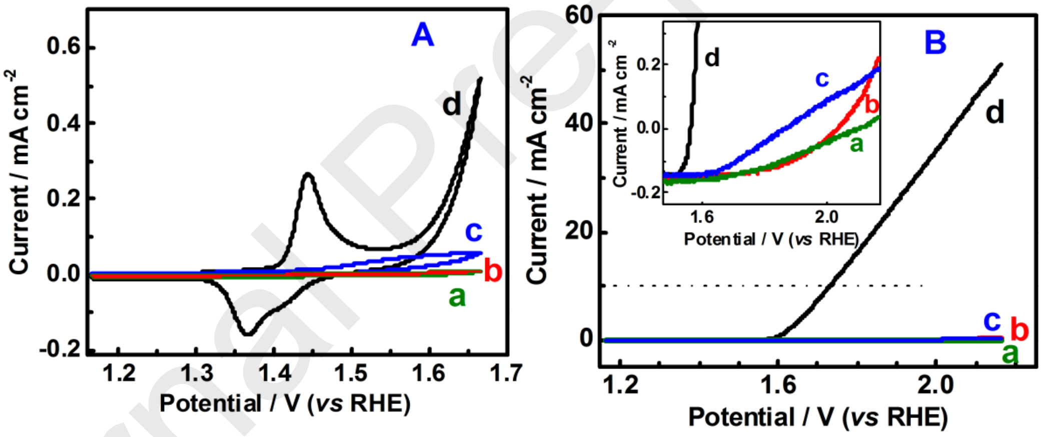

Fig. 10.A. Cyclic voltammetry of GC (a), GC/Nf (b), GC/Nf/Mn-Hfchce (c) and GC/Nf/Ni-Hfchce (d) electrodes in 0.1 M KOH with scan rate of 20 mVs^{-1}. **10.B.** LSV of GC-RDE (a), GC-RDE/Nf (b), GC-RDE/Nf/Mn-Hfchce (c) and GC-RDE/Nf/Ni-Hfchce (d) electrodes in 0.1 M KOH with scan rate of 5 mV s^{-1} and a rotation rate of 1600 rpm.

[67]

Table 1. Crystallographic data for complexes **1** and **2**

Parameters	1	2
Empirical formula	$C_{28}H_{32}N_6NiO_4S_4$	$C_{30}H_{30}MnN_6O_4S_4$
Formula weight	703.54	721.78
Crystal system	Orthorhombic	Orthorhombic
Space group	*P b c a*	*P b c n*
T (K)	120(2)	293(2)
λ, Mo Kα (Å)	0.71073	0.71073
a (Å)	15.5285(6)	18.5123(4)
b (Å)	10.7224(4)	14.2140(3)
c (Å)	19.5674(9)	12.6694(2)
α (º)	90	90
β (º)	90	90
γ(º)	90	90
V, ($Å^3$)	3258.0(2)	3333.75(11)
Z	4	4
ρ_{calcd} (g/cm^3)	1.434	1.438
μ (mm^{-1})	0.895	0.691
F(000)	1464	1728
θ range for data collections(º)	2.460-26.668°	3.88- 28.05
Index ranges	$-17 \leq h \leq 19$, $-11 \leq k \leq 13$, $-24 \leq l \leq 23$	$-24 \leq h \leq 25$, $-19 \leq k \leq 19$, $-17 \leq l \leq 16$
No. of reflections collected	10083	49141
No. of independent reflections	3392 (R_{int} = 0.0270)	4417 (R_{int} = 0.0335)
Data/restrains/parameters	3392 / 0 / 201	4417 / 0 / 204
Goodness-of-fit on F^2	1.091	1.097
R_1^a, wR_2^b [(I>2σ(I)]	0.0493, 0.1464	0.0533, 0.1228
R_1^a, wR_2^b (all data)	0.0564, 0.1558	0.0698, 0.1303
Largest difference in peak /hole ($e.Å^{-3}$)	0.482, -1.186	-0.349, -0.392
CCDC	1412088	1905731

$^aR_1 = \Sigma||F_o| - |Fc||\Sigma|F_o|$;

$^bR_2 = [\Sigma w\,(|F^2{}_o| - |F^2{}_c|)^2/\Sigma w|F^2{}_o|^2]^{1/2}$

Table 2. Selected interatomic distances & angles for **1**

Bond length (Å)			Bond angle (º)		
	(Exp)	(Cal.)		(Exp)	(Cal.)
Ni-O(1)	2.051(17)	1.909	O(1)-Ni-N(1)	89.3(8)	90.0
Ni-N(1)	2.084(2)	1.945	O(1)#1-Ni-N(1)	90.6(8)	90.0
Ni-N(2)	2.134(2)	2.643	O(1)-Ni-N(2)#1	100.4(8)	106.4
S(1)-C(7)	1.698(3)	1.707	O(1)#1-Ni-N(2)#1	79.5(8)	73.5
S(2)-C(8)	1.798(3)	1.834	O(1)-Ni-N(2)#1	100.4(8)	106.4
O(1)-C(6)	1.252(3)	1.279	N(1)-Ni-N(2)	92.0(8)	90.2
N(2)-N(3)	1.391(3)	1.378	N(1)#1-Ni-N(2)	87.9(8)	90.2
N(2)-C(7)	1.322(3)	1.324	C(7)-S(2)-C(8)	104.1(15)	104.0
N(3)-C(6)	1.325(3)	1.329	C(6)-O(1)-Ni	113.0(16)	123.6
O(2)-C(1)	1.370(5)	1.369	C(7)-N(2)-N(3)	112.0(2)	112.6
O(2)-C(4)	1.364(4)	1.362	C(7)-N(2)-Ni	142.0(19)	151.1

Table 3. Selected interatomic distances and angles for **2**

Bond length (Å)			Bond angle (º)		
	(Exp)	(Cal.)		(Exp)	(Cal.)
Mn(01)- O(2)	2.172(15)	2.180	O(2)- Mn(01)-O(2)	106.2(9)	94.8
Mn(01)- O(2)	2.172(15)	2.182	O(2)- Mn(01)-N(2)	73.4(6)	69.7
Mn(01)- N2	2.260(19)	2.400	O(2)- Mn(01)-N(2)	92.2(6)	70.6
Mn(01) -N(2)	2.260(19)	2.402	N(2)- Mn(01)-N(2)	156.3(10)	144.1
Mn(01)- N(3)	2.281(2)	2.237	O(2)- Mn(01)-N(3)	163.2(7)	169.4
S(1)-C(7)	1.687(3)	1.669	O(2)- Mn(01)-N(3)	90.5(7)	95.7
S(2)-C(7)	1.774(3)	1.760	N(2)- Mn(01)-N(3)	107.8(7)	111.6
S(2)-C(8)	1.797(3)	1.841	N(2)-C(7)-S(1)	126.3(19)	123.8
O(2)-C(6)	1.250(3)	1.254	C(6)- O(2)- Mn(01)	116.4(14)	122.0
O(1)-C(1)	1.360(3)	1.380	N(2)-C(7)-S(2)	110.5(18)	108.7
C(7)-N(2)	1.319(3)	1.390	N(1)- N(2)- Mn(01)	108.8(13)	108.5
N(2)- N(1)	1.387(2)	1.327	C(6)- N(1)- N(2)	119.0(17)	120.5

Table 4. Inter and intramolecular interactions [Å and º] for **1**

D-H···A	d(D-H)	d(H···A)	d(D···A)	<(DHA)
N(3)-H(3N)···S(1)	0.78(5)	2.38(4)	2.834(2)	119(3)
C(1)-H(1A)···S(1)#2	0.95	3.02	3.676(4)	127.1
C(5)-H(5A)···S(2)#1	0.98	2.73	3.656(3)	157.6
C(5)-H(5A)···O(1)	0.98	2.42	3.090(3)	125.5
C(8)-H(8B)···S(1)	0.99	2.66	3.167(4)	111.9
C(10)-H(10A)···S(2)	0.95	2.97	3.783(3)	145.0
C(10)-H(10A)···O(2)#3	0.95	2.65	3.240(4)	120.8
C(13)-H(13A)···S(1)#4	0.95	2.79	3.458(3)	128.0
C(14)-H(14A)···O(1)	0.95	2.58	3.046(3)	110.2

Symmetry transformations used to generate equivalent atoms:

#1 -x+1,-y+1,-z+1 #2 -x+1/2,y-1/2,z #3 x,y+1,z #4 -x+1/2,-y+1,z-1/2

Table 5. Inter and intramolecular interactions [Å and º] for **2**

D-H···A	d(D-H)	d(H···A)	d(D···A)	<(DHA)
C(8)-H(8B)···S(1)	0.97	2.76	3.225(3)	110.2
N(1)-H(1)...S(1)	0.78(3)	2.38(3)	2.859(2)	121(2)
C(1)-H(1A)...O(2)#2	0.92(3)	2.62(3)	3.452(3)	151(3)

Symmetry transformations used to generate equivalent atoms:

#1 -x+1,y,-z+1/2 #2 x,-y+2,z+1/2

[68]

Graphical Abstract (Picture)

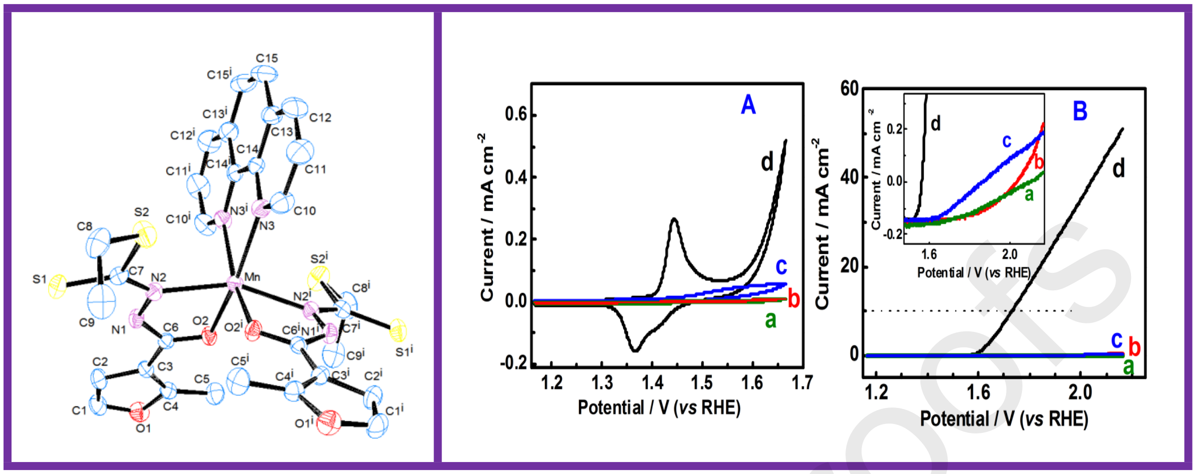

[69]

Graphical Abstract (Synopsis)

Two new complexes [Ni(Hfchce)$_2$(py)$_2$] (**1**) and [Mn(Hfchce)$_2$(*o*-phen)] (**2**) with [N'-(2-furan-3-carbonyl)hydrazine]-carbodithioic acid ethyl ester (H$_2$fchce) have been synthesized containing *o*-phen/ pyridine as coligand. Both complexes are paramagnetic and have a distorted octahedral geometry. In complex **1**, nickel centre is coordinated through one hydrazine nitrogen atom, one carbonyl oxygen atoms of two ligand moieties and two pyridine nitrogen atoms. Coordination environment of Mn(II) center in complex **2** is fulfilled by two uininegative bidentate ligands using hydrazine nitrogen, carbonyl oxygen and two nitrogen atoms of *o*-phen coligand. The arrangement of pyridine is *trans* in complex **1** while in complex **2** *o*-phen makes *cis* chelate ring, such an arrangement possibly makes complex **2** have much more distorted geometry than complex **1**. Complexes **1** and **2** are fluorescent and upon their excitation at 251 and 2263 nm, exhibit emissions at 292 and 285 nm, cm^{-1}, respectively. TG-DTA of complexes **1** and **2** indicate that the metal is converted into its metal oxide at very high temperature. Complexes **1** and **2** have efficient activity towards electrochemical water oxidation in the 0.1 M KOH. TD-DFT prediction of the experimental absorption spectrum matches very well, and from those theoretical calculations the assignment of the character of these transitions can be proposed.

[70]